

## The Effect of the Drying Process on the Properties of Bacterial Cellulose Films from *Gluconacetobacter hansenii*

Vanessa M. Vasconcellos<sup>a,b</sup>, Cristiane S. Farinas<sup>\*a,b</sup>

<sup>a</sup>Graduate Program of Chemical Engineering, Federal University of São Carlos, 13565-905, São Carlos, SP, Brazil

<sup>b</sup>Embrapa Instrumentation, Rua XV de Novembro 1452, 13560-970, São Carlos, SP, Brazil

[cristiane.farinas@embrapa.br](mailto:cristiane.farinas@embrapa.br)

Bacterial cellulose (BC) is a polymeric material that presents unique structural and mechanical properties, high crystallinity, biocompatibility, and biodegradability. All these excellent properties make BC attractive for various biotechnological applications, ranging from biomedical to electronic devices. However, the cultivation conditions to produce BC as well as the downstream processing steps can affect the properties of BC films by modifying the microstructure of the material. This paper reports on the effect of drying method on BC films produced by *Gluconacetobacter hansenii* using two different procedures (oven drying at 50°C and freeze-drying). Structural changes in the BC films were evaluated using scanning electron microscopy (SEM), thermogravimetric analyses (TGA), X-ray diffraction (XRD), and Fourier-Transform Infrared (FT-IR). The two samples were visually different, as the oven dried BC was transparent while the freeze-dried BC was whitish. SEM micrographs showed that the samples had similar interweaving, but the freeze-dried material presented a higher porosity while oven dried presented collapsed fibers, leading to a volume reduction of the film. The analysis of the thermal stability showed that the films have a similar degradation profile, starting the process of degradation at 319 °C for the oven and at 325 °C for the freeze-dried samples. The BC films showed also similar crystallinities (85%), although their diffractograms exhibit different peaks suggesting that the drying process changed the percentage of I<sub>α</sub>/I<sub>β</sub> polymorphs of the films, which was corroborated by the FT-IR results. These differences in the BC films characteristics submitted to different drying procedures can have an impact on their mechanical properties and water absorption capability, thus potentially influencing the type of possible applications.

### 1. Introduction

The bacterial cellulose (BC) is a polymeric material that presents remarkable properties as nanostructure, high crystallinity, capacity of chemical modifications, biocompatibility, biodegradability, high mechanical strength and capacity for water retention, slow capacity for water evaporation, non-toxicity, and ability to be molded 3-dimensional and with chemical modifications structures during biosynthesis. In face of all these excellent properties, the BC becomes attractive for various biotechnological applications including biomedical, cosmetic, food, pulp, paper, optical, electrical, magnetic, BC membranes and sewage purification (Iguchi et al., 2000). BC is produced mainly by the acid bacteria *Gluconacetobacter*, such as *G. xylinus* and *G. hansenii*, by cultivation in a liquid medium rich in carbohydrates, chemically defined or complex, under stirring or static condition (Esa et al., 2014). The current challenges limiting the application of BC in a broader and larger scale is related to bioprocess developments to increase its production. The process used to produce BC affects directly its properties and consequently its application. The effects of cultivation type (static or agitated; batch or fed batch process), the different bacterial strains and the culture medium (complex or industrial waste) on the BC properties has been widely studied. Besides, the downstream processing treatment of the BC can also impact the final characteristics of the material. However, how the drying process affects the properties of BC still needs to be further investigated, since most of the studies compare the properties of the film produced under different cultivations conditions using a unique drying process or during the preparation of BC composites (Hu et al., 2014; Zeng et al., 2014a). The aim of this work was to evaluate how the drying process of BC affects its properties. For this purpose BC films were produced by *G. hansenii* under static cultivation,

followed by purification step and then dried under two different procedures, oven dried or freeze-dried. Both resulting BC films were then fully characterized by microscopic, thermogravimetric, X-ray and FT-IR analysis.

## 2. Materials and methods

### 2.1 BC Synthesis, purification and drying process

The bacteria used in this work was the *Gluconacetobacter hansenii* (ATCC 23769). The methodology for the synthesis of BC was divided into four steps: activation, pre-inoculum, inoculum and cultivation. The culture medium used was the Hestrin and Schramm (1954) and the pH was adjusted to 5.0 with a citric acid solution. In the activation phase the bacteria was inoculated into HS-agar medium and incubated at 30°C until growth. The next step was the pre-inoculum in liquid medium, in which the grown cells on the agar was removed and transferred to 20 mL of fresh HS medium. After three days, 10 mL of pre-inoculum was added into 40 mL of fresh medium and was incubated for more three days. The cultivation for BC production started by inoculating 4% of the inoculum into fresh HS medium and incubating it for 7 days. The whole process took place at 30 °C under static conditions. The purification was carried out by separating the BC from the medium and boiling (~95°C) in a 1% (w/v) sodium hydroxide solution for 60 min for removal of cells and medium embedded in the cellulose film. After purification, the film was rinsed with distilled water until neutral pH. The BC films were either oven dried (Oven FANEM 502, Brazil) at 50 °C on a silicon surface for 48 hours, until constant weight (Oven-dried BC) or frozen at -30 °C and then freeze dried (Freeze Drier LIOBRAS 101, Brazil) on petri dishes (Freeze-dried BC).

### 2.2 Characterization Analyzes

Scanning Electron Microscopy SEM analysis was performed on a microscope JEOL (Model JSM-6510) equipped with a secondary electron detector (SEI) and operated at 10 kV. For these analyses, all samples were attached to aluminum stubs using adhesive carbon tape and then coated with gold (Leica Sputter Coater - SCD050 Coating system). The BC films were fixed directly onto the carbon tape. Bacterial sample was prepared on a slice of glass, using for fixing a Karnovsky solution. For dehydration, the samples were washed with acetone solution at different concentrations and freeze dried. The samples used for all analyses were randomly picked from the BC films.

Thermogravimetric analysis (TGA) of BC samples was carried out using a TA instruments (TGA Q500 V6.3 build 189) using sample of about 7 mg in a platinum sample holder. Each sample was scanned over a temperature range from ambient temperature to 600°C at a heating rate of 10 °C/min under nitrogen atmosphere with a sample flow rate 50 mL/min and balance flow rate 50 mL/min to avoid sample oxidation. Thermogravimetric derivative (DTG) was also obtained from the data.

The X-ray diffraction (XDR) was performed with a high-resolution X-ray diffractometer (Shimadzu 6000) with a Ni-filtered Cu K $\alpha$  (1,540562 Å) radiation source operated at voltage 30 Kv and 30 mA electric current. The dried BC samples were scanned from 5° to 85° 2 $\theta$  range with a step of 0,02°, a step time of 4,0 sec and scan speed 2°/min. The % Crystallinity was calculated by two methods, the Height peak method (%C<sub>H</sub>) Eq(1)(Segal et al., 1959) and the Area peak method Eq(2) (%C<sub>A</sub>) (Park et al., 2010). A peak fitting program (OringiPro) was used, assuming pVoigt functions for each crystalline peak and a broad peak around 22° assigned to the amorphous phase. The equations used are below:

$$\%C_H = \frac{I_{002} - I_{AM}}{I_{002}} \times 100 \quad (1)$$

$$\%C_A = \left(1 - \frac{A_A}{A_T}\right) \times 100 \quad (2)$$

Where  $I_{002}$  is the maximum intensity of the lattice diffraction (2 $\theta$  of 22° to 23°) and  $I_{AM}$  is that of the amorphous material where the intensity is minimum (2 $\theta$  of 18° to 19°),  $A_A$  is the area relative to the amorphous fraction and  $A_T$  is the total area of the original diffractogram.

Attenuated Total Reflectance Fourier-Transform Infrared (ATR-FTIR) spectroscopy analyses was carried out on the BC films on a Vertex 70 FTIR spectrometer (Bruker), equipped with a Universal ATR accessory, using 32 scans and a resolution of 4 cm<sup>-1</sup>, over the range 4000-400 com<sup>-1</sup> and their background was recorded with an empty cell for each sample. The spectra's were normalized and cellulose I $\alpha$  fraction (Kataoka and Kondo, 1999) and I $\alpha$ , I $\beta$  content (Bi et al., 2014) were calculated using the peak heights at 750 and 710 cm<sup>-1</sup> as showed the following equations:

$$I_{\alpha} \text{ fraction} = \frac{A_{750}}{A_{750} + A_{710}} \quad (3)$$

$$I_{\alpha} = 2.55 * I_{\alpha} \text{ fraction} - 0.32 \quad (4)$$

### 3. Results and discussions

#### 3.1 Synthesis, Purification and Drying Process of BC

Morphological characterization of *G. hansenii*, the crude BC film and the purified BC oven dried was carried out using SEM. From Figure 1, it is possible to show that the purification process was effective in removing bacteria intertwined in the cellulose film and traces of culture medium. The purification process also increased the BC films transparency.

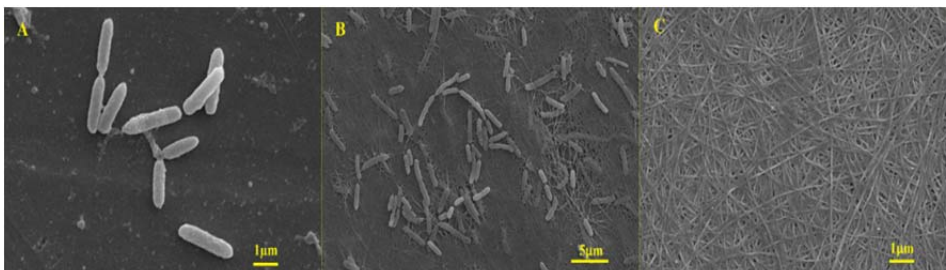


Figure 1: SEM micrographs of *G. hansenii* (ATCC- 23769) (A), BC films after 7 days of static cultivation at 30 °C before (B) and after (C) purification with NaOH 1 % (w/v) for 60 min at 100 °C.

The BC samples produced and purified were subjected to two different drying processes: oven dried or freeze-dried. Figure 2 shows the appearance of the samples at the end of the different drying processes. It can be seen that the oven dried BC (Figure 2A) has transparency while the freeze-dried BC (Figure 2B) does not, looking like a “Styrofoam”. The structure of the cellulose membranes was investigated with higher resolution using SEM (Figure 2C and 2D), in which the BC fibers dispersion and the interfacial adhesion are shown. Similarly to previous reports, BC films show a hierarchical structure with pores of different sizes from macro to micro scale. It is notable that both samples show similarity between the interweaving of the fibers. However the freeze-dried BC has a higher porosity while the oven dried sample the fibers are more collapsed, presenting a lower porosity.

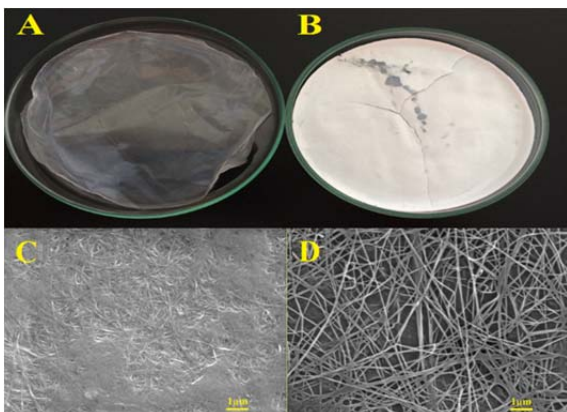


Figure 2: BC films oven dried (A) and freeze dried (B) and SEM micrographs of BC films oven dried (C) and freeze dried (D).

The thickness of the oven-dried membrane was much lower than the freeze-dried,  $12 \pm 2$  and  $627 \pm 84$  μm, respectively. A simple visual observation does not provide information about the crosslink forming the film, but probably the reduced volume of oven dried BC is related to the collapse of the polymer chains that form the structural network of the membrane. The diversity of applications and biological functions of BC membranes are based on their distinct morphology, and the intertwining of the fibers in films is responsible for its considerable mechanical strength and water absorption capacity. Zeng et al. (2014b) confirmed these differences evaluating three different drying processes: room temperature drying, freeze drying and supercritical CO<sub>2</sub> drying, and found out that mechanical properties, such as penetration depth, hardness, and also water absorption capacity were modified by the drying process, and each process favors a specific characteristic.

### 3.2 BC Characterization

The TGA and DTG curves of bacterial cellulose are presented in Figure 3. It is possible to observe that oven-dried BC and freeze-dried BC have similar behavior in relation to heat degradation, showing the typical single step thermal degradation profile. Three stages of mass loss were associated with the TGA curves. A first stage below 150 °C, with less than 10% weight loss, is associated with the release of water and other volatile compounds present in the film. A second stage, at range 250 - 450 °C, shows a severe weight loss. This event is associated with the process of cellulose degradation, involving depolymerization, dehydration and decomposition of glycosyl units followed by the formation of a charred residue (Mohammadkazemi et al, 2015). The third stage extends to the usual ending test temperature at 600°C. The single step confirms that the adopted purification process promoted the removal of all contaminants.

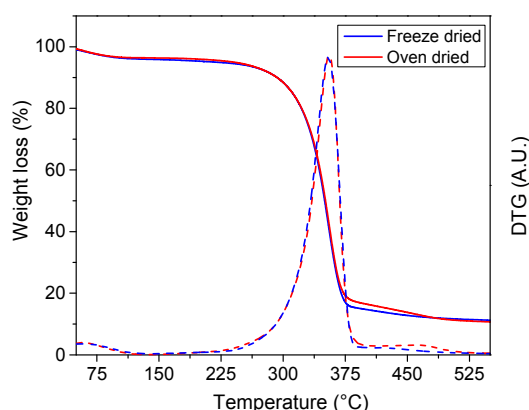


Figure 3: TGA (---) and DTG (- - -) of cellulose produced by *G. hansenii* in HS medium under different drying processes.

The results of temperature of  $T_{\text{onset}}$  and main DTG peak are listed in Table 1. It was observed no significant differences between BC samples under the drying processes studied. This indicates that the drying process did not affect the thermal degradation. The high thermal resistance of BC with a decomposition temperature around 355°C is in agreement with previous studies using alkaline treatment and similar drying processes, freeze dried (Mohite and Patil, 2014) and oven dried (Zeng et al., 2014b).

Table 1: Details of TGA, DTG, DRX and FT-IR characterization of BC films under different drying processes

| BC Sample    | $T_{\text{onset}}$ (°C) | Main DTG peak temp. (°C) | %C <sub>H</sub> | %C <sub>A</sub> | $I_{\alpha}$ fraction | $I_{\alpha}$ | $I_{\beta}$ |
|--------------|-------------------------|--------------------------|-----------------|-----------------|-----------------------|--------------|-------------|
| Oven dried   | 319.6                   | 355.4                    | 84              | 68              | 0.35                  | 57.2         | 42.8        |
| Freeze dried | 325.2                   | 354.5                    | 85              | 64              | 0.37                  | 62.3         | 37.7        |

The BC is a semi-crystalline material and its structure is composed of cellulose I, predominantly by polymorph  $I_{\alpha}$  (Zeng et al., 2014b). To compare the microstructure changes in the BC oven dried and freeze-dried, X-ray diffraction was used. The diffractograms of the samples are presented in Figure 4A. The peaks found for the two samples only suggest the presence of cellulose I, peak 1 (~15°) corresponds to the 100 plane of cellulose  $I_{\alpha}$  or to the  $1\bar{1}0$  plane of cellulose  $I_{\beta}$ , peak 2 (~17°) corresponds to the 010 plane of cellulose  $I_{\alpha}$  or to the 110 plane of cellulose  $I_{\beta}$  and peak 3 (~23°) corresponds to the 110 plane of cellulose  $I_{\alpha}$  or to the 200 plane of cellulose  $I_{\beta}$  (Wada et al, 2001). The samples have different peaks and intensity, each diffracted peak presents only one contribution of the corresponding diffractions of the phase  $I_{\alpha}$  and  $I_{\beta}$ , which is difficult to estimate due to overlapping of the planes reflections. The diffractograms also reveals the presence of the amorphous region in BC ( $I_{\text{am}} \sim 20^\circ$ ). The % crystallinity (%C) was calculated using two different methods and the results are presented in Table 1. The %C<sub>H</sub> showed no difference between the samples dried by different processes and both have high crystallinity (%C<sub>H</sub>~85%), when the peak area was used there was also no significant difference in crystallinity between the drying processes, but the %C<sub>A</sub> value was reduced in almost 20% (%C<sub>A</sub>~65%). The difference of the values between the methods was expected, since the height method is an empirical measurement to allow relative rapid comparison between samples. However, there is some reasons that it

should not be used as a method for estimating the amount of crystalline and amorphous material in a cellulose sample, as the height used for amorphous fraction is not aligned with the maximum height of the amorphous peak, only the highest crystalline peak is used in the calculation and only the height is taken into account being that width also plays a very important role (Park et al., 2010).

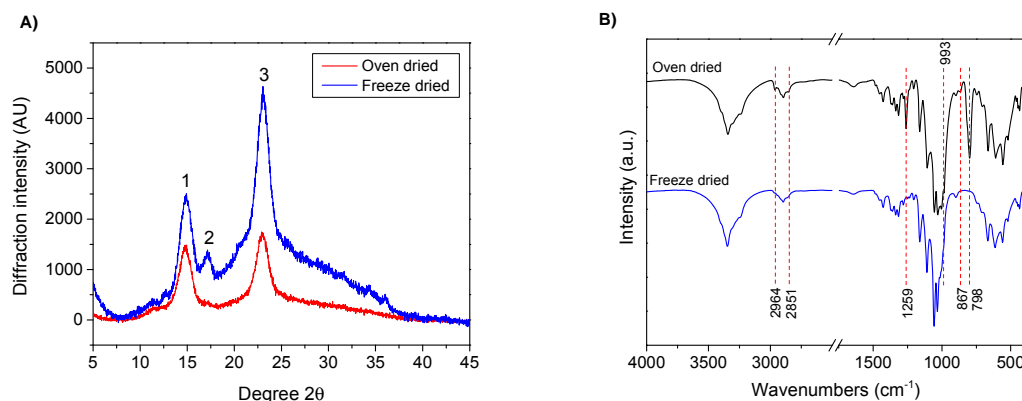


Figure 4: X-ray diffractogram (A) and FTIR vibrational spectra (B) of BC produced by *G. hansenii* in HS medium under different drying processes.

The results suggest that different drying methods are not influencing the crystallinity of BC, but the methods are changing the proportion of polymorphs I<sub>α</sub>/I<sub>β</sub>. Zeng et al. (2014b) found similar crystallinity results and peaks for films to dried at room temperature and freeze-dried.

The FT-IR spectra of oven- and freeze-dried cellulose are presented in Figure 4B. It is possible to observe that the films have similar profile, the absorption bands at 798, 867, 1035, 1637, 2851, 2919, 2964 and 3350 cm<sup>-1</sup> in the spectra characterize the material as bacterial cellulose. The region between the bands 3600-3000 cm<sup>-1</sup> corresponds to hydrogen bond O-H stretching, hydrogen bonds for cellulose I include two intramolecular bonding namely, O(2)H-O(6) bonding (3405-340 cm<sup>-1</sup>) and O(3)H-O(5) bonding (3340-3375 cm<sup>-1</sup>) and one intramolecular bonding O(6)H-O(3) (3230-3310 cm<sup>-1</sup>) (Fan et al., 2012). The presence of the bands 1429, 1163, 1111, 897 cm<sup>-1</sup> also characterizes the formation of cellulose I (Nelson and O'Connor, 1964). These results indicate that the drying process used was not able to transform cellulose I into II, but the increased intensity of the band around 993 cm<sup>-1</sup> in the oven-dried film suggests the formation of a new crystal structure with a cellulose II characteristic (Yue et al., 2015). The appearance of cellulose II may be related to the process of film purification with sodium hydroxide, as the appearance of cellulose II after the alkaline purification process has been reported by Zeng et al. (2014b).

It is possible to observe some changes around 800-950 cm<sup>-1</sup> band. This region is sensitive to the amount of amorphous cellulose, i.e. broadening of this band indicates higher amount of disordered structure (Ang et al., 2012; Proniewicz et al., 2002) and the increase in the intensity of the 2900 cm<sup>-1</sup> band in the oven-dried cellulose spectrum are indications that this film is more crystalline (Ciolacu et al., 2011). The efficiency of the purification process also can be confirmed through the FT-IR spectro, due to the absence at 1642 cm<sup>-1</sup> band which relate to amide presence (Zeng et al., 2014b).

Table 1 shows the I<sub>α</sub> fraction and the amount of α and β polyforms of cellulose I. The results indicate that freeze dried process slightly increased the cellulose I<sub>α</sub> amount in the BC film, suggesting that the dried process would affect the formation of two distinct crystalline variation in the crystalline structure of cellulose I: meta stable state cellulose I<sub>α</sub> and stable state cellulose I<sub>β</sub> (Nelson and O'Connor, 1964). Bi and co-workers (2014) reported that different strains can produce cellulose film with different concentrations of cellulose I<sub>α</sub> in agitation culture. The drying technique can modify the chemical bonds, as the disorder of cellulosic structure may be caused by the different arrangements in the angles around β-glycoside linkages and hydrogen bond rearrangement (Proniewicz et al., 2002).

#### 4. Conclusions

The results of this work using two different drying processes allowed the production of different BC films with different structural properties. Such materials could be used to create novel complex nanocomposites with different applications. The oven drying and freeze-drying methods did not affect the thermal stability and crystallinity of the film, but modified the transparency, porosity and polymorphs composition of BC films, what

can interfere directly in the potential applications. A better understanding of how the drying process affects the properties of the BC films may contribute for the development of novel biotechnological materials for different applications.

### Acknowledgments

The authors would like to thank Embrapa, CNPq (Process 401182/2014-2), CAPES (Process 88881.134591/2016-01), and FAPESP (Processes 2014/19000-3 and 2016/10636-8) (all from Brazil) for their financial support.

### Reference

- Ang T. N., Ngoh G. C., Chua A. S. M., Lee M. G., 2012, Elucidation of the Effect of Ionic Liquid Pretreatment on Rice Husk Via Structural Analyses, *Biotechnology for Biofuels*, 5, 10.
- Bi J. C., Liu S. X., Li C. F., Li J., Liu L. X., Deng J., Yang, Y. C., 2014, Morphology and Structure Characterization of Bacterial Celluloses Produced by Different Strains in Agitated Culture, *Journal of Applied Microbiology*, 117(5), 1305-1311.
- Ciolacu D., Ciolacu F., Popa, V. I., 2011, Amorphous Cellulose - Structure and Characterization, *Cellulose chemistry and technology*, 45(1), 13.
- Esa F., Tasirin S. M., Rahman, N. A., 2014, Overview of Bacterial Cellulose Production and Application. 2nd International Conference on Agricultural and Food Engineering (Cafe 2014) - New Trends Forward, 2, 113-119.
- Fan M., Dai D., Huang B., 2012, Fourier Transform Infrared Spectroscopy for Natural Fibres, *Fourier Transform-Materials AnalysisInTech*.
- Hestrin, S. and Schramm, M., 1954, Synthesis of Cellulose by *Acetobacter-xylinum*, *Biochemical Journal*, 58(2), 345-352.
- Hu, W. L., Chen, S. Y., Yang, J. X., Li, Z. and Wang, H. P., 2014, Functionalized Bacterial Cellulose Derivatives and Nanocomposites, *Carbohydrate Polymers*, 101, 1043-1060.
- Iguchi M., Yamanaka S., Budhiono A., 2000, Bacterial Cellulose - A Masterpiece of Nature's Arts, *Journal of Materials Science*, 35(2), 261-270.
- Kataoka Y., Kondo, T., 1999, Quantitative Analysis for the Cellulose I $\alpha$  Crystalline Phase in Developing Wood Cell Walls, *International Journal of Biological Macromolecules*, 24(1), 37-41.
- Mohammadkazemi F., Azin M., Ashori, A., 2015, Production of Bacterial Cellulose Using Different Carbon Sources and Culture Media, *Carbohydrate Polymers*, 117, 518-523.
- Mohite B. V., Patil, S. V., 2014, Physical, Structural, Mechanical and Thermal Characterization of Bacterial Cellulose by *G-hansenii* NCIM 2529, *Carbohydrate Polymers*, 106, 132-141.
- Nelson M. L., O'Connor R. T., 1964, Relation of Certain Infrared Bands to Cellulose Crystallinity and Crystal Latticed Type, Part I, *Journal of Applied Polymer Science*, 8(3), 1311-1324.
- Park S., Baker J. O., Himmel M. E., Parilla P. A., Johnson D. K., 2010, Cellulose Crystallinity Index: Measurement Techniques and their Impact on Interpreting Cellulase Performance, *Biotechnology for Biofuels*, 3, 10.
- Proniewicz L. M., Paluszkiwicz C., Weselucha-Birczynska A., Baranski A., Dutka, D., 2002, FT-IR and FT-Raman Study of Hydrothermally Degraded Groundwood Containing Paper, *Journal of Molecular Structure*, 614(1-3), 345-353.
- Segal, L., Creely, J. J., A.E. Martin, J. and Conrad, C. M., 1959, An Empirical Method for Estimating the Degree of Crystallinity of Native Cellulose Using the X-Ray Diffractometer.
- Wada M., Okano T., Sugiyama J., 2001, Allomorphs of Native Crystalline Cellulose I Evaluated by Two Equatorial D-Spacings, *Journal of Wood Science*, 47(2), 124-128.
- Yue Y., Han J., Han G., Zhang Q., French A. D., Wu Q., 2015, Characterization of Cellulose I/II Hybrid Fibers Isolated from Energycane Bagasse During the Delignification Process: Morphology, Crystallinity and Percentage Estimation, *Carbohydrate polymers*, 133, 438-447.
- Zeng M. L., Laromaine A., Feng W. Q., Levkin P. A., Roig, A., 2014a, Origami Magnetic Cellulose: Controlled Magnetic Fraction and Patterning of Flexible Bacterial Cellulose, *Journal of Materials Chemistry C*, 2(31), 6312-6318.
- Zeng M. L., Laromaine A., Roig, A., 2014b, Bacterial Cellulose Films: Influence of Bacterial Strain and Drying Route on Film Properties, *Cellulose*, 21(6), 4455-4469.